The structural and optical properties of Cu_2O films electrodeposited on different substrates

2005 Semicond. Sci. Technol. 20 44

(http://iopscience.iop.org/0268-1242/20/1/007)

INSTITUTE OF PHYSICS PUBLISHING SEMICONDUCTOR SCIENCE AND TECHNOLOGY

Semicond. Sci. Technol. **20** (2005) 44–49 doi:10.1088/0268-1242/20/1/007

The structural and optical properties of Cu_2O films electrodeposited on different substrates

Y L Liu[1], Y C Liu[2,4], R Mu[3], H Yang[2], C L Shao[2], J Y Zhang[1], Y M Lu[1], D Z Shen[1] and X W Fan[1]

[1] Key Laboratory of Excited State Process, Changchun Institute of Optics, Fine Mechanics and Physics, Chinese Academy of Sciences, Changchun 130022, People's Republic of China
[2] Center for Advanced Optoelectronic Functional Material Research, Northeast Normal University, Changchun 130024, People's Republic of China
[3] Center for Photonic Materials and Devices, Fisk University, Nashville, TN37208, USA

E-mail: ycliu@nenu.edu.cn

Received 2 July 2004, in final form 31 October 2004
Published 3 December 2004
Online at stacks.iop.org/SST/20/44

Abstract

Cuprous oxide films were successfully electrodeposited onto three different substrates through the reduction of copper lactate in alkaline solution at pH = 10. The substrates include indium tin oxide film coated glass, n-Si wafer with (001) orientation and Au film evaporated onto Si substrate. The substrate effects on the structural and optical properties of the electrodeposited films are investigated by *in situ* voltammetry, current versus time transient measurement, *ex situ* x-ray diffraction, scanning electron microscopy, UV–vis transmittance and reflectance and photoluminescence techniques. The results indicate that the choice of substrate can strongly affect the film morphology, structure and optical properties.

1. Introduction

Cuprous oxide, a p-type direct-gap semiconductor with a bandgap energy of 2.1 eV, has been regarded as one of the most promising materials used for optoelectronic applications recently [1–21]. The increase in its attractiveness has several reasons: (1) Cu_2O is a potential photovoltaic material due to the low cost, non-toxicity and the natural abundance of the base material [5–7]. (2) Excitons created in Cu_2O have been shown as suitable candidates for Bose–Einstein condensate because of the large exciton binding energy of 150 meV [8–10]. Bose–Einstein condensation of excitons could occur when the high density excitation is used with a pulsed laser. (3) Cu_2O is a basic compound forming superconducting materials. Furthermore, Cu_2O is one of the few oxide semiconductors that are p-type. It is also known that Cu_2O related materials such as $CuAlO_2$ and $SrCu_2O_2$ families are transparent conductive oxides (TCO) exhibiting p-type conductivity [22–25]. And these TCOs have electronic structure similar to Cu_2O, except for considerably larger energy gaps. The nature of the p-type conductivity of Cu_2O is originated from the presence of Cu vacancies which form an acceptor level above the valence band.

Several methods including thermal oxidation, chemical oxidation, anodic oxidation, vacuum evaporation and electrodeposition have been used to prepare Cu_2O films. Among these, electrodeposition is the simplest and the most convenient method. It also has several advantages over others, such as low processing temperature, higher deposition rates, controllable film thickness and morphology. Uniform films can be formed on various substrates with complex shapes and employed with inexpensive equipment. It has been demonstrated that electrodeposition is an effective method for growing Cu_2O films [18, 26–29].

In order to explore the potential of using Cu_2O for various optoelectronic device applications, it is interesting to deposit Cu_2O films onto different substrates. Examples are (a) Cu_2O deposited on the conventional semiconductor Si may be used in electronic devices and (b) Cu_2O grown on ITO can be used

[4] Author to whom any correspondence should be addressed.

in solar energy cells. Electrodeposition of Cu_2O on Si has been rarely reported, only recently Switzer *et al* reported the epitaxial electrodeposition of Cu_2O on p-type single crystal silicon [18].

In this paper we report the success of using the electrodeposition technique to form Cu_2O films on different substrates and conduct a detailed structural and optical investigation of Cu_2O films.

2. Experimental details

2.1. Film deposition

The electrochemical deposition of Cu_2O was conducted in an electrolyte solution consisting of 0.4 M cupric sulfate and 3 M lactic acid at pH = 10 adjusted by the addition of sodium hydroxide.

The substrates are ITO coated glass, (001) oriented n-Si and thin Au film evaporated onto a Si substrate. Prior to the deposition of the ITO, the glass substrate was ultrasonically cleaned in an acetone bath and rinsed with doubly distilled water. The Si substrate was immersed in a 5% HF solution for oxide removal followed by rinsing with doubly distilled water. The Au film was obtained by evaporating Au onto a Si substrate. And then the film was annealed at 300 °C for 30 min under a N_2 atmosphere. This is considered to be a crucial step to ensure a good binding between the Au film and Si surface and to enhance the crystal quality of Au film. Upon annealing, XRD shows that the Au film on Si wafer has a (111) preferred orientation. The growth of Cu_2O was carried out in a classic three-electrode cell.

For the deposition, each substrate was used as a working electrode and a large area of Pt was used as a counter electrode. An Ag/AgCl electrode was employed as a reference electrode. All potentials reported in the paper were referring to the reading from the working electrode versus the Ag/AgCl reference electrode. Electrodeposition was controlled by a potentiostat/galvanostat. The data acquisition was obtained by a PC. Deposition was carried out potentiostatically at −300 mV, which is chosen for deposition of pure phase of Cu_2O. The solution was kept at a constant temperature of 60 °C during deposition with a controlled temperature water bath. All the films in this study were grown under the same condition except the substrate material.

2.2. Characterization techniques

X-ray diffraction (XRD) spectra were measured using a rotating anode x-ray diffractometer with Cu $K_{\alpha 1}$ radiation of 1.541 Å. The surface morphology of the film was investigated by a Hitachi S4200 field-emission scanning electron microscopy. A Shimadzu UV-350 double beam spectrophotometer was used to measure transmission and reflectance spectra for the films grown on ITO substrate. A Hitachi MPF-4 spectrophotometer was used to measure the reflectance spectra of the films grown on the opaque substrates. The room temperature photoluminescence spectra (RT PL) of the films were obtained by using the UV Labran Infinity Spectrophotometer made by JY Company, which is excited by the 488 nm line of an Ar^+ laser.

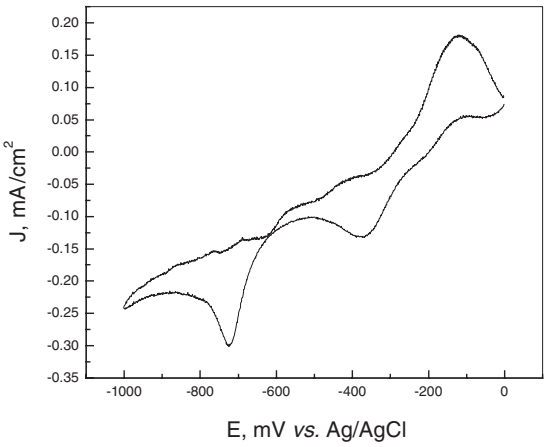

Figure 1. Cyclic voltammograms for a bare Pt electrode at 50 mV s^{-1} acquired in the electrolyte containing 0.4 M cupric sulfate and 3 M lactic acid with pH = 10 adjusted by adding sodium hydroxide.

3. Results and discussion

3.1. Growing kinetics

A cyclic voltammogram for an uncoated Pt electrode from the prepared electrolyte containing 0.4 M cupric sulfate and 3 M lactic acid at pH = 10 is shown in figure 1. Two prominent voltammetric oscillations with peaks at about −375 and −725 mV were observed. Both oscillations represent two reduction processes. The first oscillation started at about −200 mV and is known as a diffusion controlled process corresponding to the reduction of Cu^{2+} to Cu^+. The second has a high negative potential and can be attributed to the reduction of Cu^+ to Cu^0. The cyclic voltammogram indicated that when the copper lactate solution had no NaOH at pH = 2, only one broad reduction curve with a peak at −180 mV was observed. It suggests that this peak should be the direct reduction Cu^{2+} to Cu. Therefore, it is believed that the increase in pH by adding NaOH serves two purposes. First, Cu_2O deposition can be expected to occur selectively, which ensures the single phase electrodeposition of Cu_2O at an appropriate potential. The other is to prevent the disproportion reaction of Cu_2O in low pH aqueous solution. By complexing with lactate ion, Cu^{2+} can be stabilized in the solution when the pH is increased. The formation of the Cu_2O from alkaline solution containing copper ions follows the reaction:

$$2Cu^+ + 2OH^- \rightarrow Cu_2O + H_2O.$$

Figure 2 shows the current–time transients at a potential of −300 mV versus Ag/AgCl during deposition on various substrates. For all the substrates, a nucleation and growth mechanism can be seen. For the film grown on ITO, electrical current increases gradually during deposition after nucleation has occurred in the ITO surface. In the cases of films growth on both Si and Au substrates, the monitored current decreases monotonically. It is believed that the continuous decrease in current reflects different deposition mechanisms. In the case of Si substrate, the decrease of the current may be the result of the formation of an amorphous SiO_2 layer on the Si surface [18], which limits the current. For the Au surface, on the other hand, the decrease in measured current is due to the resistivity increase as a result of Cu_2O film formation.

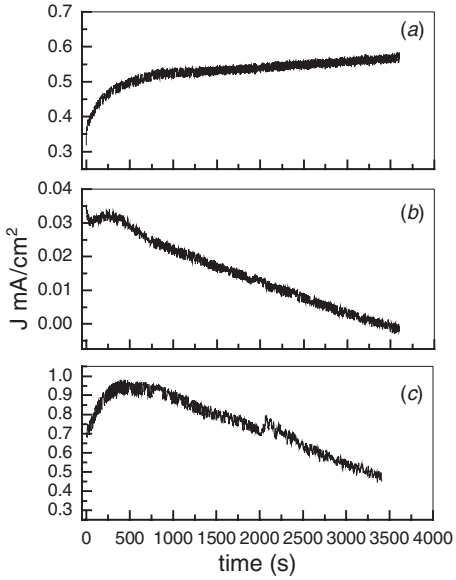

Figure 2. Current versus time transients for the film grown on (*a*) ITO coated glass, (*b*) (001) oriented n-Si and (*c*) Au substrate during the electrodeposition.

3.2. Structure and morphology of Cu_2O films

Cu_2O films potentiostatically grown on ITO, Si and Au substrates have been analysed by XRD. Their diffraction patterns are shown in figure 3. All three kinds of films show single phase Cu_2O diffraction peaks with no other traces of Cu or CuO observable. For the film grown on ITO glass, four diffraction peaks are observed and identified as Cu_2O (110), (111), (200) and (220) directions. (JCPDS card file no 5-0667) The strongest peak in the XRD spectrum represents the (111) crystal direction. The film grown on n-type (100) Si substrate shows a similar x-ray pattern to that grown on ITO, but it has broader and weaker diffraction peaks. In the case of Au substrate, highly (200) oriented Cu_2O film was deposited and the peaks are much narrower than the films grown on the other two substrates. The lattice parameter for the three Cu_2O films is the same and it is in agreement with the standard value of $a = 4.27$ Å.

In the case of Cu_2O film grown on Si, the relatively broad and weak XRD peaks may suggest nano-sized Cu_2O particle formation. According to the Scherrer formula, the calculated grain size of the Cu_2O evaluated from the dominant (111) diffraction peak is 12 nm.

According to the XRD results, the choice of substrate materials plays a crucial role in the formation of Cu_2O. ITO glass used here is a polycrystalline isotropic material with no preferred orientation. Thus, the Cu_2O film grown on this substrate shows (111) preferential orientation at pH = 10, which may suggest that the fastest growth direction of Cu_2O is along the (111) direction. The n-type Si substrate has a (100) orientation with a lattice parameter of $a = 5.43$ Å. The mismatch of the Cu_2O/Si system calculated from $|a_{\text{film}} - a_{\text{substrate}}|/a_{\text{substrate}}$ is about 21.4%. The large mismatch makes it difficult to grow Cu_2O epitaxially as a result of Cu_2O film with the same preferred orientation as that grown on isotropic substrate. Another reason may be that an amorphous SiO_2 layer had formed at the interface between

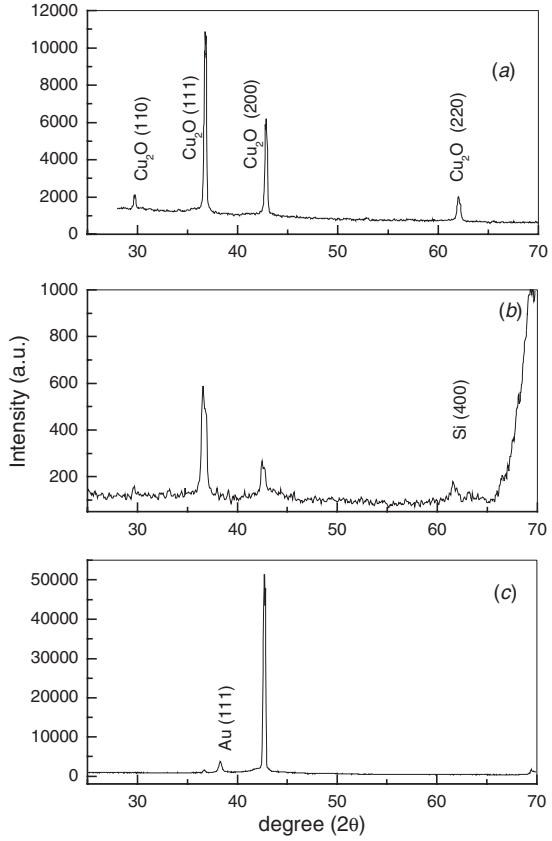

Figure 3. X-ray patterns for Cu_2O films deposited on (*a*) ITO coated glass, (*b*) (001) oriented n-Si and (*c*) Au substrate.

Si and solution even before the deposition occurs. Thus, no preferred orientation is expected. For the same reason the Cu_2O film grown on Si substrate shows lower crystal quality and smaller grain size.

In the case of Au surface, the calculated lattice mismatch between Au and Cu_2O crystals is about 4.7%. Contrary to our expectation, an intense (200) diffraction peak was observed for the film grown on Au surface instead of the (111) direction. A similar result has been reported when Cu_2O grew with a (100) orientation when Cu_2O film surpassed a critical thickness on single (111) Au substrate as described by Switzer [17].

The surface morphologies of the Cu_2O films grown on different substrates are analysed with a SEM technique and the images are shown in figure 4. Clearly, the grains of pyramidal shape are corresponding to the (111) growth direction with an ITO substrate. The average grain size is ~ 2 μm. The Cu_2O film grown on Si substrate also consists of four-sided pyramid crystals, but the size of the crystals is much smaller, less than 100 nm. However, the grain size illustrated in the SEM images is larger than that the XRD estimated size. A possible explanation is that the result obtained from XRD measurements reflects the crystalline domain size rather than the physical particle size suggesting the observed particles may contain multi-domains within the particle or polycrystalline particles. Cu_2O film grown on Au surface has a (100) orientation. A relatively smooth and rather compact Cu_2O polycrystalline film was also observed. The large micron sized Cu_2O particles indicate a good crystal quality of the Cu_2O film.

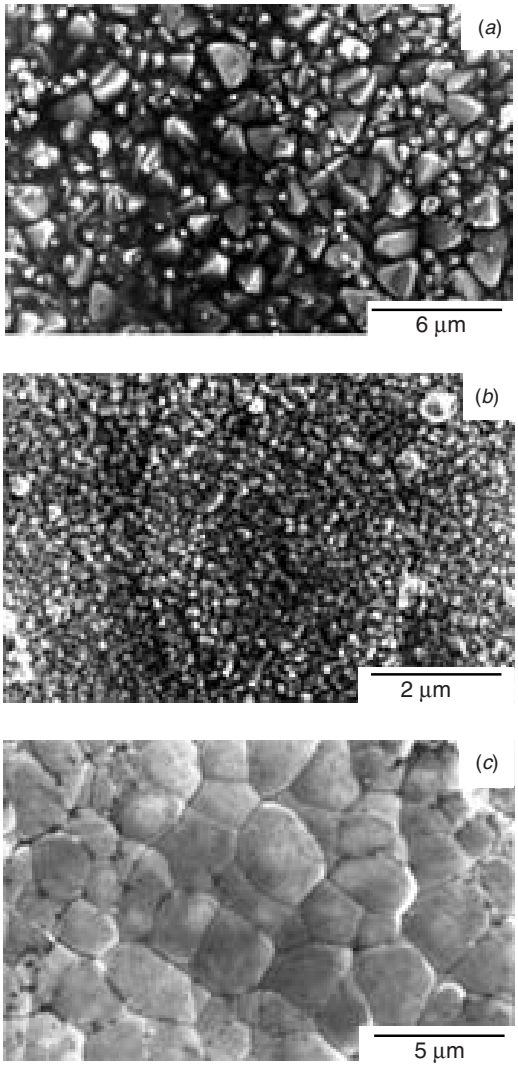

Figure 4. Surface SEM photos of Cu_2O film grown on (*a*) ITO coated glass, (*b*) (001) oriented n-Si, and (*c*) Au substrate.

From the analyses, it can be seen that the SEM shapes of Cu_2O are in good agreement with XRD results.

3.3. Optical properties

The transmission and reflection spectra were measured for Cu_2O films grown on ITO, Si and Au surfaces and are illustrated in figure 5. In order to determine the optical band gap of the Cu_2O film, both transmittance T and reflectance R were converted to absorbance α, in terms of $\alpha = \frac{1}{d}\ln\frac{1-R}{T}$, and $\alpha + R + T = 1$. The direct optical gap E_g was determined by extrapolating the function

$$(\alpha E)^2 = B(E - E_g)$$

on to the horizontal axis (energy), where B is a proportionality constant which reflects the integrality of the crystal lattice. Figure 6 shows the graph of $(\alpha E)^2$ versus E for the film grown on ITO and Au. The absorption edges of Cu_2O grown on ITO and Au are 2.10 and 2.14 eV, respectively, characteristic of bulk Cu_2O. The slope of B for Cu_2O grown on Au is much steeper than that grown on ITO, which implies that the film

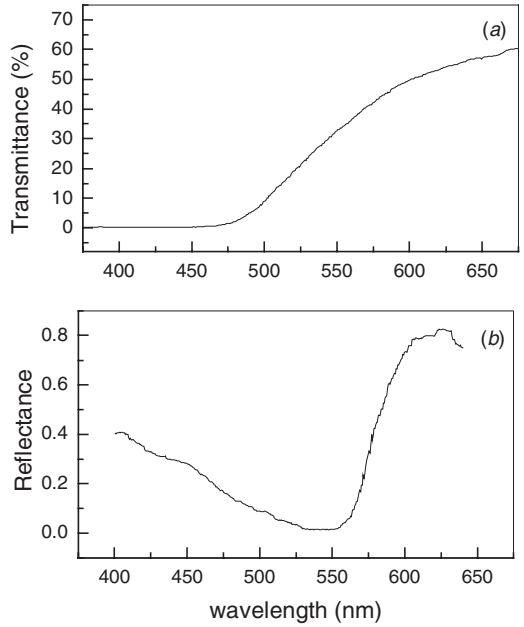

Figure 5. Transmittance spectrum of the film grown on ITO coated glass (*a*) and reflectance spectrum of the film grown on Au film evaporated onto a Si substrate (*b*).

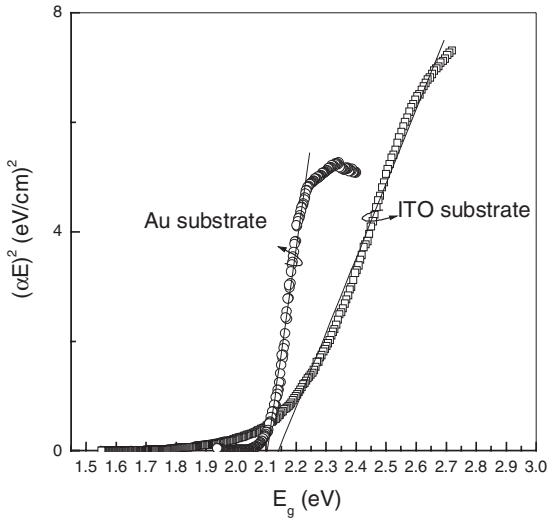

Figure 6. Plots of $(\alpha E)^2$ versus E to determine the energy of the direct optical absorption edges for Cu_2O films grown on: (□) ITO coated glass, (○) Au substrate.

grown on Au substrate has better crystal structure than that grown on ITO.

The absorption of Cu_2O grown on Si is broad and weak. There is also a very weak but identifiable absorption feature at ∼480 nm (2.58 eV) observed. The blueshift should be caused by the quantum confinement effect. A similar blueshift has been seen by Yang *et al* [30]. It is difficult to determine the optical gap of the film. Lack of sharpness in absorption spectra has also been observed in the optical absorption spectra for Cu_2O nanoparticles prepared by other authors [1, 19, 20]. The reason for the weak absorption feature may be the result of increasing light scattering caused by the decrease in grain size and the increase in size distribution of the nanocrystals.

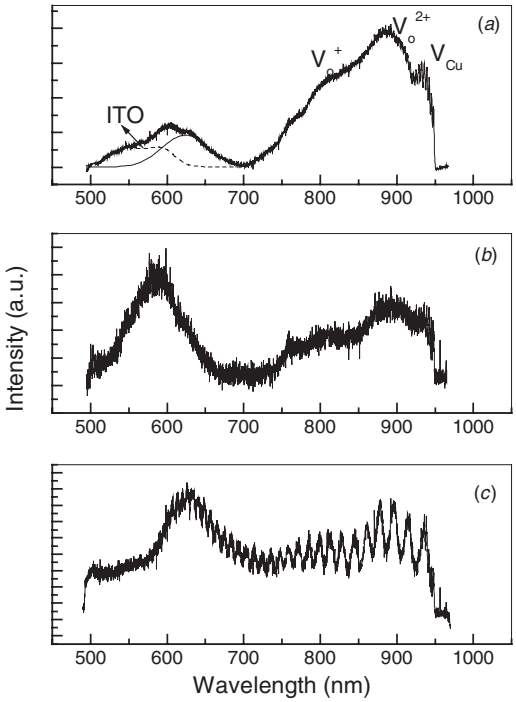

Figure 7. Room temperature photoluminescence for the film grown on (*a*) ITO coated glass, (*b*) (001) oriented n-Si, and (*c*) Au substrate. Curve (*a*) was simulated into two profiles and the high-energy curve denoted by the dashed line shown is from the ITO substrate.

The room temperature (RT) photoluminescence spectra of Cu_2O film grown on all three substrates were also studied using the 488 nm line of an Ar^+ laser, as shown in figure 7. All the photoluminescence spectra in the 500–950 nm region are composed of two major components. The peak observed in the visible region (∼590–625 nm) is associated with the near band emission, while a broad band with three luminescence peaks in the near infrared region is related to different active trapping centres [21, 31, 32].

It is known that the energy minimum of the conduction band and energy maximum of the valance band in Cu_2O are nondegenerate, and located at the zone centre. Since both of the bands have even parity, electric dipole transitions between the two states are forbidden. An exciton formed from these two bands has to annihilate through other means, thus as electric quadrupole transitions, or via phonon assisted transitions [21]. The crystal structure of Cu_2O includes two molecules per unit cell and group theoretical analysis suggests that the phonons have symmetries Γ_{25}^-, Γ_{15}^-, Γ_{12}^- and Γ_{25}^- at the Γ point in this material. At room temperature, only one broad near band luminescence is observed. At the high energy side, the PL spectrum obtained from Cu_2O grown on ITO glass shows an asymmetric broad emission band, which can be fit with two symmetric peaks. Among them, the peak illustrated by the dashed line at $\lambda \sim 580$ nm is due to the emission of the ITO glass, which was also observed from bare ITO glass. The photoluminescence peak at 626 nm (1.98 eV) with the FWHM of 177 meV was attributed to the exciton emission of Cu_2O. The line shape of the PL spectrum of Cu_2O film grown on Au is similar to the emission of the film grown on ITO film. The sample grown on Au film shows a peak at 629 nm (1.97 eV) with a FWHM of 182 meV. The fluctuation observed in this PL spectrum is caused by the Fabry–Perot interference effect for light reflected at the gold interface and the surface, indicating a good film quality.

Compared to the bulk Cu_2O, an obviously blueshift emission of the near band emission with a peak at 590 nm (2.10 eV) was observed for the nanoparticle Cu_2O grown on Si substrate. It may be argued that the blueshift is caused by the quantum confinement of exciton photogenerated inside the nanoparticle. The FWHM of the PL peak is 222 meV, and the broadening of the PL peak is in agreement with the small grain size.

The photoluminescence band in the near band range of 700–950 nm may be assigned to the emission of different defect centres. For film grown on ITO and Si substrates, three luminescence centres were observed. The luminescence band at $\lambda \sim 930$ nm is attributed to V_{Cu}, those at $\lambda \sim 802$ and 880 nm are attributed to V_o, the former is doubly ionized oxygen vacancies V_o^{2+}, and the latter is singly ionized ones V_o^{2+} [21]. For the film grown on Au surface only one weak peak is observed at ∼880 nm due to V_o^{2+}. Thus, it further shows that the film grown on Au film has better quality.

4. Conclusion

In summary, we have successfully grown Cu_2O films on three substrate surfaces. The growth dynamics, structural and optical properties of Cu_2O films on different substrates (Si, ITO and Au film) were investigated. Cu_2O crystals with microsized pyramidal shape were grown on ITO substrate. Nanosized and pyramidal shaped Cu_2O particles were formed on Si substrate. The pyramidal morphology of Cu_2O particles grown on ITO and Si substrate is consistent with the observation of (111) preferred orientation from XRD. The film grown on Au substrate shows a (100) orientation with much better crystallinity. RT PL measurements have been conducted. PL spectra show two spectral emission profiles. One is the near band gap emission in the visible region. The other is the emission in the infrared region due to the different defect centres. An obvious blueshift of the near band emission is observed for the nanocrystalline Cu_2O formed on Si substrate, which may be due to the quantum confinement effects of excitons in Cu_2O nanoparticles.

Acknowledgments

This work was supported by the Program of CAS Hundred Talents, the National Natural Science Foundation of China (60176003), Excellent Young Teacher Foundation of the Ministry of Education of China, and the Foundational Excellent Researcher to Go beyond Century of the Ministry of Education of China.

References

[1] Borgohain K, Murase N and Mahamuni S 2002 *J. Appl. Phys.* **92** 1292
[2] Okamoto Y, Ishizuka S, Kato S, Sakurai T, Fujiwara N, Kobayasshi H and Akimoto K 2003 *Appl. Phys. Lett.* **82** 1060

[3] Ishizuka S, Kato S, Akimoto Y and Akimoto K 2002 *Appl. Phys. Lett.* **80** 950
[4] Mishina E D, Nagai K and Nakabayashi S 2001 *Nano Lett.* **1** 401
[5] Fernando C A N, De Silva L A A, Mehra R M and Takahashi K 2001 *Semicond. Sci. Technol.* **26** 433
[6] Chen Z Z, Shi E W, Zheng Y Q, Li W J, Xiao B and Zhuang J Y 2003 *J. Cryst. Growth* **249** 294
[7] Mathew X, Mathews N R and Sebastian P J 2001 *Sol. Energy Mater. Sol. Cells* **70** 277
[8] Snoke D 1996 *Science* **273** 1351
[9] Merizzi A, Masse M and Fortin E 2001 *Solid State Commun.* **120** 419
[10] Johnson K and Kavoulakis G M 2001 *Phys. Rev. Lett.* **86** 858
[11] Mukhopadhyay A K, Chakraborty A K, Chatterjee A P and Lahiri S K 1992 *Thin Solid Films* **209** 92
[12] Bohannan E W, Shumsky M G and Switzer J A 1999 *Chem. Mater.* **11** 2289
[13] Lu D L and Tanaka K I 1996 *J. Electrochem. Soc.* **143** 2105
[14] de John P E, Vanmaekelvergh D and Kelly J J 1999 *Chem. Mater.* **11** 3512
[15] Barton J K, Vertegel A A, Bohannan E W and Switzer J A 2001 *Chem. Mater.* **13** 952
[16] Mahalingam T, Chitra J S P, Rajiendran S and Sebastian P J 2002 *Semicond. Sci. Technol.* **17** 565
[17] Switzer J A, Kothari H M and Bohannan E W 2002 *J. Phys. Chem.* B **106** 4027
[18] Switzer J A, Liu R, Bohannan E W and Ernst F 2002 *J. Phys. Chem.* B **106** 12369
[19] Kellersho A, Knozinger E, Langel W and Iersig M G 1995 *Adv. Mater.* **7** 652
[20] Deki S, Akamastsu K, Yano T, Mizuhata M and Kajinami A 1998 *J. Mater. Chem.* **8** 1865
[21] Ito T and Masumi T 1997 *J. Phys. Soc. Japan.* **66** 2185
[22] Kawazoe H, Yasukawa M, Hyodo H, Kurita M, Yanagi H and Hosono H 1997 *Nature* **389** 938
[23] Kudo A, Yanagi H, Hosono H and Kawazoe H 1998 *Appl. Phys. Lett.* **73** 220
[24] Robertson J, Peacock P W, Towler M D and Needs R 2002 *Thin Solid Films* **411** 960
[25] Ohta H, Orita M, Hirano M, Yagi I, Ueda K and Hosono H 2002 *J. Appl. Phys.* **91** 3074
[26] Poizot P, Hung C H, Nikiforov M P, Bohannan E W and Switzer J A 2003 *Electrochem. Solid State Lett.* **6** C21
[27] Katayama J, Ito K, Matsuoka M and Tamaki J 2004 *J. Appl. Electrochem.* **34** 687
[28] Ernst F and Switzer J 2003 *Z. Mt. kd.* **94** 259
[29] Mahalingham T, Chitra J S P, Chu J P and Sebastian P J 2004 *Mat. Lett.* **58** 1802
[30] Yang M and Zhu J J 2003 *J. Cryst. Growth* **256** 134
[31] Prevot B, Carabatos C and Sieskind M 1972 *Phys. Status Solidi* A **10** 455
[32] Gastev S V, Kaplyanskii A A and Sokolov N S 1982 *Solid State Commun.* **42** 389